

# Influence of MHD and porous media on peristaltic transport for nanofluids in an asymmetric channel for different types of walls

Qabas K. Jawad, Ahmed M. Abdulhadi\*

*Department of Mathematics, College of Science, University of Baghdad, Baghdad, Iraq*

*(Communicated by Javad Vahidi)*

---

## Abstract

This paper's aim is to discuss the influence of nanoparticles and porous media, and magnetic field on the peristaltic flow transport of a couple of stress fluids in an asymmetric channel with different waveforms of non-Newtonian fluid. Initially, Mathematical modelling of the 2-D and two directional flows of a couple of stress fluids with a nanofluid is first given and then simplified beneath the hypothesis of long wavelength and low Reynolds number approximation. After making these approximations, we will obtain associated nonlinear differential equations. Then the exact solutions of the temperature distribution, nanoparticle concentration, velocity, stream function, and pressure gradient will be calculated. Finally, the results that we obtained illustrate graphically.

Keywords: porous media, magnetic field, peristaltic flow, asymmetric channel, nanofluids particles, couple stress  
2020 MSC: Primary 90C33; Secondary 26B25

---

## 1 Introduction

Nanofluids are those liquids which contain a very tiny amount of nanoparticles which are about a thousand of a human hair thin. These liquids compared to other liquids created using different theories, have a higher single-phase heat transfer coefficient, particularly for laminar flow. This makes them more desirable than other fluids, such as heat transfer fluids, in many heat transfer applications, such as microelectronics, pharmaceutical processes utilizing fuel cells, hybrid-powered engines, engine cooling, domestic refrigerators, heat exchangers in machining, and the reduction of boiler flue gas temperature. Compared to the base fluid, they have improved thermal conductivity and the convective heat transfer coefficient. Regarding liquids, they were crucial for numerous applications in daily life, therefore they so occupied a considerable area among researchers [13, 2, 4].

Choi also clarified the peristaltic flow characteristics of nanofluids. Following that, other studies explored the phenomenon of nanofluids utilizing various flow geometries [9, 8] the peristalsis mechanism, which is caused by the continual contraction and expansion of the elastic organ, tubular structure accommodating fluid, occurs frequently in a number of psychological processes. peristalsis successfully moves materials over long distances and through complicated routes.

Applications of peristalsis can be seen throughout the human body, including the movement of chyme through the colon, the transfer of lymphatic vessels, heart-lung devices, and peristaltic pumps, Latham [14] and Shapiro [17] first

---

\*Corresponding author

*Email addresses:* qabas.kadem1203a@sc.uobaghdad.edu.iq (Qabas K. Jawad), ahm6161@yahoo.com (Ahmed M. Abdulhadi)

presented a fluid dynamical analysis of peristalsis for 2D Newtonian fluids. The effect of Hall current on the peristaltic motion of Maxwell fluid moving through porous material was discussed by Hayat [12]. Ali study .s on the analysis of heat transport across curved channels is found in [5]. The peristaltic was explored by Tripathi [18]. investigated the peristaltic motion of viscous liquids while taking into account heat transmission and porosity along the channel's limited length. A few research on the subject are also listed in the references [1, 7, 3, 11].

The term "porous medium" refers to a collection of solid bodies or a solid material made up of porous structures that have enough space between them or around them to allow liquid to pass through or around them. Permeability and porosity are two of the most distinguishing qualities of porous media, while there are many others. Porous media can be identified by their spatial properties such as hardness, permeability, and porosity. Many different materials, including man-made ones like cement, natural ones like rocks, and biological tissues like bone and wood, can be found in porous media. Various applications use porous media. Life in the scientific and engineering disciplines of materials science, petroleum engineering, construction engineering, earth sciences, petroleum geology, and geophysics. Additionally, liquids move through porous media due to friction between the liquid and the walls of the medium's structure, which hinders the liquid's motion. The porous medium utilized in this procedure will be referred to as filters, as well [15, 10, 6].

In a previous paper [16] we studied and analyzed the same problem but with a sinesidol boundary in, the present paper different types of boundaries will be considered.

## 2 Mathematical formulation

The motion of the peristaltic flow of an electrically conductive incompressible stress fluid in a two-dimensional channel of width  $d_1 + d_2$  is taken into account. The movement of the flow is stimulated by sine wave trains that will travel at a constant speed  $c$  along the walls of the channel. We will choose a rectangular coordinate system for the channel with  $x$  along the centre line of the channel and  $y$  transverse to it. The left wall temperature is maintained at  $T_1$  and the right wall has a temperature  $T_0$ . Therefore, the velocity field of the two-dimensional flow and two directional the forms will be  $V = [U(X, Y, T), V(X, Y, T), 0]$ . Assuming that the fluid is subject to a constant tangential magnetic field  $B_0$ . It is assumed that the Reynolds number and the induced magnetic field are very small and therefore the induced magnetic field can be neglected. When the fluid is transferred to the magnetic field, two main physical effects will be generated, the first will cause an electric field  $E$  in the flow, and under the assumption that there is no excess charge density and therefore  $\nabla B = 0$ . Since the induced magnetic field is neglected, it means that  $\nabla E = 0$  and therefore the electric field The stimulus is not mentioned. The second effect is the Cally dynamics in nature, which is the Lorenz force ( $J \times B$ ), where  $J$  is the density of the current. And that this force affects the fluid and modifies the movement. This will result in the transfer of energy from the electromagnetic field to the fluid.

## 3 Expressions for different wave types:

The boundary wall equation are

- Triangular wave

$$h_1 = 1 + a \left\{ \frac{8}{\pi^3} \sum_{m=1}^{\infty} \frac{(-1)^{m+1}}{(2m-1)^2} \sin[2\pi(2m-1)x] \right\}$$

$$h_2 = -d - b \left\{ \frac{8}{\pi^3} \sum_{m=1}^{\infty} \frac{(-1)^{m+1}}{(2 * m - 1)^2} \text{Sin}[2\pi(2m-1)x + \phi] \right\}$$

-Trapezoidal wave

$$h_1 = 1 + a \left\{ \frac{32}{\pi^2} \sum_{m=1}^{\infty} \frac{\sin \left[ \frac{\pi}{3}(2m-1) \right]}{(2m-1)^2} \text{Sin}[2\pi(2m-1)x] \right\}$$

$$h_2 = -d - b \left\{ \frac{32}{\pi^2} \sum_{m=1}^{\infty} \frac{\text{Sin} \left[ \frac{\pi}{9}(2m-1) \right]}{(2m-1)^2} \text{Sin}[2\pi(2m-1)x + \phi] \right\}$$

-square wave

$$h_1 = 1 + a \left\{ \frac{4}{\pi} \sum_{m=1}^{\infty} \frac{(-1)^{m+1}}{(2m-1)} \cos[2(2m-1)\pi x] \right\}$$

$$h_2 = -d - b \left\{ \frac{4}{\pi} \sum_{m=1}^{\infty} \frac{(-1)^{m+1}}{(2m-1)} \text{Cos}[2(2m-1)\pi x + \phi] \right\}$$

-multisinusoidal wave

$$h_1 = 1 + a \sin[2n\pi x], h_2 = -d - b \sin[2n\pi x + \phi]$$

Follow, our previous paper [16] the governing equation

$$-\frac{\partial p}{\partial x} + \frac{\partial^2 u}{\partial y^2} - \frac{1}{\gamma^2} \frac{\partial^4 u}{\partial y^4} - u \left( M^2 + \frac{1}{D1} \right) - M^2 + Gr\theta + Br\phi = 0 \tag{3.1}$$

$$-\frac{\partial p}{\partial y} = 0 \tag{3.2}$$

$$\frac{1}{Pr} \frac{\partial^2 \theta}{\partial y^2} + Nb \frac{\partial \theta}{\partial y} \frac{\partial \phi}{\partial y} + Nt \left( \frac{\partial \theta}{\partial y} \right)^2 = 0 \tag{3.3}$$

$$\frac{\partial^2 \phi}{\partial y^2} + \frac{Nt}{Nb} \frac{\partial^2 \theta}{\partial y^2} = 0 \tag{3.4}$$

The identical dimensionless boundary conditions which governed the flow are defined:

$$u = -1, \frac{\partial^2 u}{\partial y^2} = 0 \text{ at } y = h_1 = 1 + a \cos 2\pi x \tag{3.5}$$

$$u = -1, \frac{\partial^2 u}{\partial y^2} = 0 \text{ at } y = h_2 = -d - b \cos(2\pi x + \phi) \tag{3.6}$$

$$\theta = 0, \phi = 0 \text{ at } y = h_1 \tag{3.7}$$

$$\theta = 0, \phi = 1 \text{ at } y = h_2 \tag{3.8}$$

The dimensionless mean flow  $Q$ , is defined:

$$Q = F + 1 + d \tag{3.9}$$

where

$$F = \int_{h_1}^{h_2} u dy$$

### 4 Solution of the problem

The aim in this section to find the exact solution for the equation (3.4) can be obtained and follows:

$$\phi(x, y) = -\frac{Nt}{Nb} \theta + a1(x)y + a2(x) \tag{4.1}$$

Where  $a1(x)$  and  $a2(x)$  are two unknown functions which can be found by using the boundary conditions. Now substitute eq.(4.1) into (3.3) we get the exact solution of eq.(4.1)

$$\theta(x, y) = \frac{a3(x)}{Pr Nb a1(x)} + a4(x)e^{-Pr Nb a1(x)} \tag{4.2}$$

Where  $a3(x)$  and  $a4(x)$  are unknown functions.

Now substitute the equation (4.2) into (4.1) the dimensionless concentration can be obtained, and is given by

$$\phi(x, y) = -\frac{Nt}{Nb} \left[ \frac{a3(x)}{Pr Nb a1(x)} + a4(x)e^{-Pr Nb a1(x)} \right] + a1(x)y + a2(x) \tag{4.3}$$

Now, to find the values of unknown function  $a1(x), a2(x), a3(x)$ , and  $a4(x)$  We need to use boundary conditions (3.7), (3.8).

By using the boundary condition for  $\theta$  and  $\phi$  on equation (4.3) it follows that

$$a1(x) = \frac{1 + \frac{Nt}{Nb}}{h_2 - h_1} \tag{4.4}$$

$$a2(x) = -h_1 \left( \frac{1 + \frac{Nt}{Nb}}{h_2 - h_1} \right) \tag{4.5}$$

To calculate the values of  $a3(x), a4(x)$  we apply the boundary condition for  $\phi$  on equation (4.2) we get

$$a3(x) = \frac{e^{-PrNba1(x)h_1}}{e^{-PrNba1(x)h_2} - e^{-PrNba1(x)h_1}} \tag{4.6}$$

$$a4(x) = \frac{1}{e^{-PrNba1(x)h_2} - e^{-PrNba1(x)h_1}} \tag{4.7}$$

Thus the exact expressions for the temperature distribution  $\theta$  and nano particle concentration  $\phi$  are given:

$$\theta(x, y) = \left( \frac{e^{-PrNba1(x)y} - e^{-PrNba1(x)h_1}}{e^{-PrNba1(x)h_2} - e^{-PrNba1(x)h_1}} \right) \tag{4.8}$$

$$\left( 1 + \frac{Nt}{Nb} \right) \left( \frac{y - h_1}{h_2 - h_1} \right) \theta(x, y) = \left( \frac{e^{-PrNba1(x)y} - e^{-PrNba1(x)h_1}}{e^{-PrNba1(x)h_2} - e^{-PrNba1(x)h_1}} \right) \tag{4.9}$$

With the help of equation (4.8) and (4.9) the solution of velocity is obtained from equation(3.1) and is defined :

$$u1 = e^{y^* s1} c1 + e^{-y^* s1} c2 + e^{y^* s2} c3 + e^{-y^* s2} c4 - \left( 16e^{-a1NbPr y} \left( Br \left( e^{a1NbPr(y+h_1)} - \dots \right) \right) \right) \tag{4.10}$$

where

$$s1 = \left( \frac{\sqrt{\gamma^2 - \frac{\sqrt{\gamma^2(-4 - 4D1M^2 + D1\gamma^2)}}{\sqrt{D1}}}}{\sqrt{2}} \right), s2 = \left( \frac{\sqrt{\gamma^2 + \frac{\sqrt{\gamma^2(-4 - 4D1M^2 + D1\gamma^2)}}{\sqrt{D1}}}}{\sqrt{2}} \right),$$

$$s3 = \left( \sqrt{2\gamma^2 - \frac{2\sqrt{\gamma^2(-4 - 4D1M^2 + D1\gamma^2)}}{\sqrt{D1}}} \right),$$

where  $c1, c2, c3$ , and  $c4$  are constant. The constants  $c1, c2, c3$ , and  $c4$  are calculated with help of boundary conditions in equation (3.5)-(3.6) The pressure is given by follows:

$$\frac{dp}{dx} = - \left( \left( e^{-((s1+s2)y)} \left( Bre^{(a1NbPr+s1+s2)y} (e^{a1NbPrh_1} - e^{a1NbPrh_2}) \right) (Nb + \dots \right) \right) \right) \tag{4.11}$$

$$\psi = -c2e^{-s1y} s1 + c1e^{s1y} s1 - c4e^{-s2y} s2 + c3e^{s2y} s2 \tag{4.12}$$

### 5 Results and discussion:

This section aims to study the effect of various factors on pressure gradient and stream function (See Figures (3.1) -(3.35)).In the current study, the value of the following default parameters was adopted for the calculations  $\phi = Pi/6, Pr = 0.9, a = 0.5, Nb = 0.3, Nt = 0.5, d = 1.8, b = 1, Gr = 0.8, Br = 0.1, Q = 2, M = 0.2, \gamma = 2.5, D1 = 1$  therefore all graphs correspond to these values unless they are specified on the appropriate graph. All the results in this section are made through plotting by using MATHEMATICA package.

### 5.1 Variation of pressure gradient triangular wave:

The behavior of pressure gradient profile for different values  $\phi, Pr, a, Nb, Nt, d, b, Gr, Br, Q, M, \gamma$  and  $D_1$  can be seen through figure (3.1)-(3.13) respectively. In the concentration  $\phi$  when  $x \in [0, 0.1]$  the pressure gradient is increasing with increasing concentration but when  $x = [0.15]$  is the reflection point and when  $x \in [0.2, 0.6]$  the pressure gradient decreases with increasing concentration then the pressure starts to increase gradually when  $x \in [0.65, 0.8]$ . Prandtl number  $Pr$  has little effect on the pressure gradient due to its appearance within limits so its effect will decrease. The amplitude of the wave number  $a$  when  $x \in [0, 0.45]$  the pressure gradient is increasing with the increasing value of the amplitude of the wave number  $a$  when  $x = [0.5]$  is the reflection point then when  $x \in [0.6, 0.8]$  the pressure gradient decreases with increasing value of the amplitude of the wave number  $a$  this happens because of the nature of the wall. The pressure gradient decreases with the increasing value of the thermophoresis parameters  $Nt$  this means that the concentration decreases due to the velocity increase, which leads to less pressure. The pressure gradient decreases with the increasing value of the magnetic parameter  $M$  because of low viscosity. In the amplitude of the wave number  $b$  when  $x \in [0, 0.35]$  the pressure gradient is increasing with the increasing value of the amplitude of the wave number  $b$  but when  $x = [0.4]$  is the reflection point and the pressure gradient decreases with increasing value of the amplitude of the wave number  $b$  when  $x \in [0.45, 0.8]$  This happens because of the nature of the wall. The pressure gradient is increasing with the increasing value of the nanoparticle Grashof number  $Br$ , the width number  $d$ , discharge  $Q$ , and the couple stress parameter  $\gamma$ . The pressure gradient is increasing with the increasing value of the local temperature Grashof number  $Gr$  This occurs as a result of the effect of the quotient multiplying the length wave in the viscosity. The pressure gradient is increasing with the increasing value of the Brownian motion parameter  $Nb$  Due to the lack of kinematic viscosity and the pressure gradient is increasing with the increasing value of the porosity parameter  $D_1$  Due to increased permeability of molecules.

The pressure gradient is increasing with the increasing value of the amplitude of the wave number  $b$  when  $x \in [0, 0.15]$  but when  $x \in [0.2, 0.4]$  the amplitude of the wave number  $b$  has little effect after that when  $x \in [0.45, 0.7]$  the pressure gradient is decreasing with an increasing value of the amplitude of the wave number  $b$  then the pressure gradient gradually increases when  $x \in [0.75, 0.8]$  This happens because of the nature of the wall. In the magnetic parameter  $M$  the pressure gradient decreases with the increasing value  $M$  because of low viscosity.

### 5.2 Stream line:

Trapping is the process of creating an internally circulating bolus of fluid through closed stream lines. This trapped bolus is then propelled forward by the peristaltic wave. Trapping for various values of  $\phi, Pr, a, Nb, Nt, d, b, Gr, Br, Q, M, \gamma$  and  $D_1$  can be seen through figure (3.14) (3.22). The stream lines for different values of the concentration  $\phi$  it has been noticed that the bolus increases in size in the upper wall tapered channel with increasing  $\phi$  but in the lower wall the bolus decreases in size with increasing  $\phi$ . The Prandtl number  $Pr$ , Brownian motion parameter  $Nb$ , and thermophoresis parameters  $Nt$  have little effect on the stream line. The stream lines for various values of The amplitude of the wave number  $a$  It's been observed that the bolus decreases size in the upper wall tapered channel with increasing  $a$  while in the lower the size of bolus increases with increasing value of  $a$ . In the amplitude of the wave number  $b$ , and the width number  $d$  the size of boulds is increasing with increasing value of  $b, d$  in upper walls and in the lower walls the size of boulds decreases with increased. values of  $b, d$ . The stream lines for different values of the local temperature Grashof number  $Gr$ , and nanoparticle Grashof number  $Br$  the size of boulds decreases with increasing of values in the upper walls but in the lower walls, the size of boulds increases with increasing values  $Gr, Br$ . The stream lines for different values of the magnetic parameter  $M$ , and the couple stress parameter  $\gamma$  increases in size in the upper wall tapered channel with increasing values  $M, \gamma$  but in the lower wall the bolus decreases in size with increasing  $M, \gamma$ . In the porosity parameter  $D_1$  the size of boulds increases with increasing values of  $D_1$  in upper walls and in the lower walls, the size of boulds decreases with increasing values of  $D_1$ .

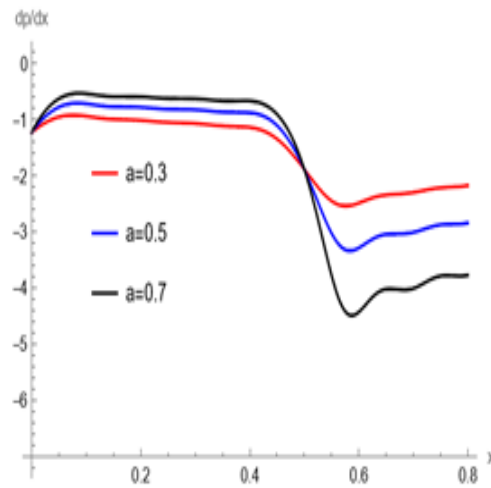


Figure 1: variation of pressure gradient  $dp/dx$  with  $x$  for different values of  $a$

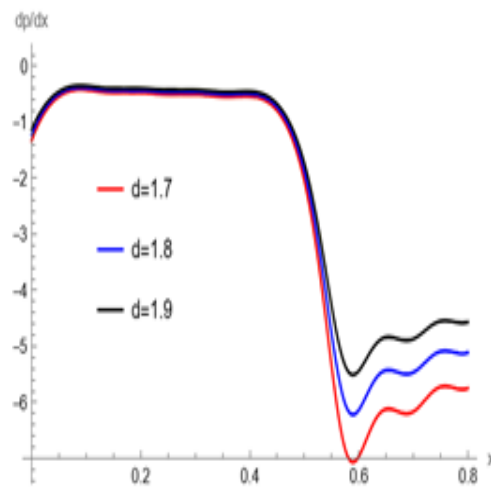


Figure 2: variation of pressure gradient  $dp/dx$  with  $x$  for different values of  $d$

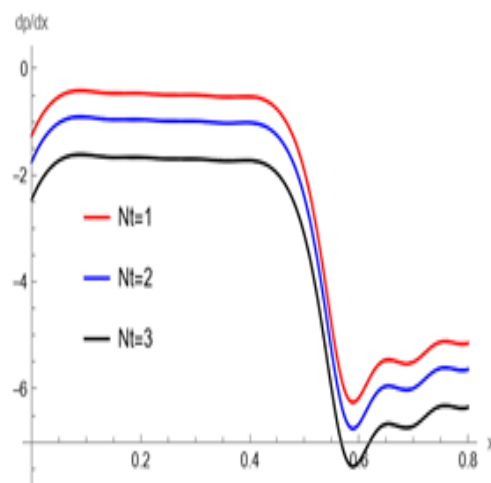


Figure 3: variation of pressure gradient  $dp/dx$  with  $x$  for different values of  $Nt$

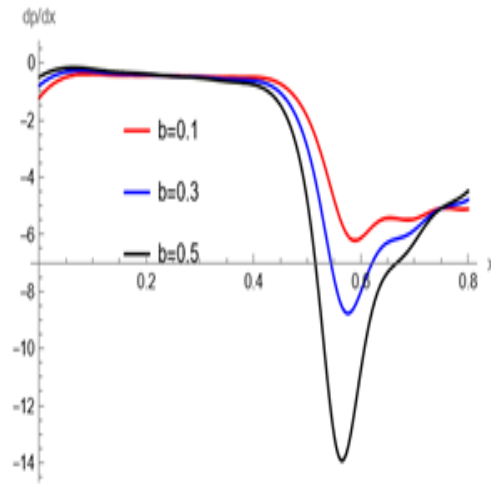


Figure 4: variation of pressure gradient  $dp/dx$  with  $x$  for different values of  $b$

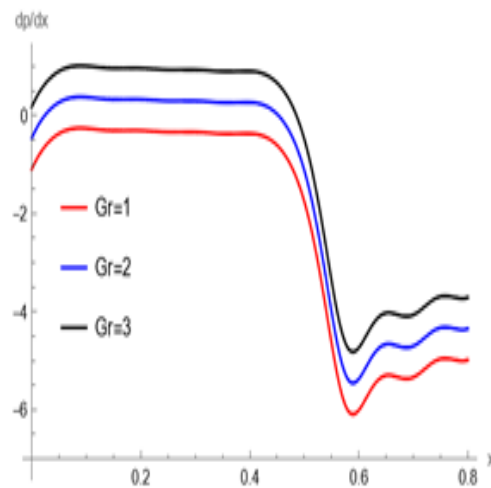


Figure 5: variation of pressure gradient  $dp/dx$  with  $x$  for different values of  $Gr$

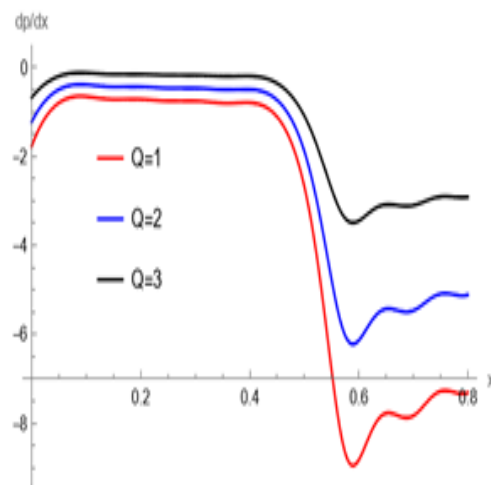


Figure 6: variation of pressure gradient  $dp/dx$  with  $x$  for different values of  $Q$

### 5.3 Variation of the pressure gradient multisinusoidal wave

The behavior of pressure gradient profile for different values  $\phi, Pr, a, Nb, Nt, d, b, Gr, Br, Q, M, \gamma$  and  $D_1$  can be seen through figure (3.26)-(3.38) respectively. The pressure gradient increases with increasing value of concentration

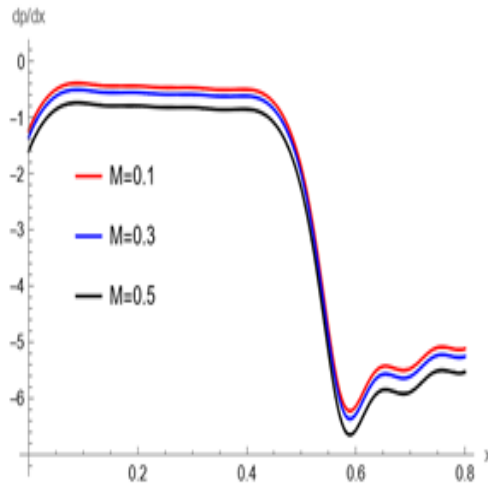


Figure 7: variation of pressure gradient  $dp/dx$  with  $x$  for different values of  $M$

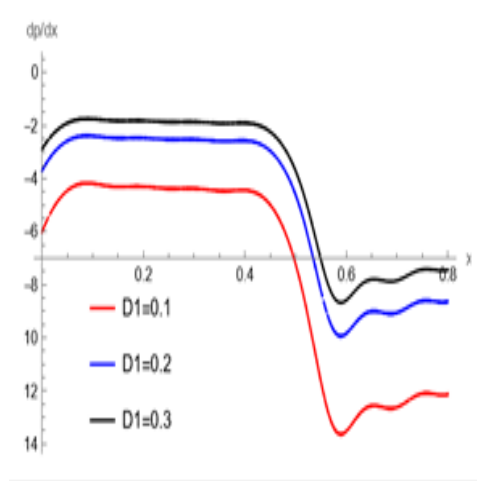


Figure 8: variation of pressure gradient  $dp/dx$  with  $x$  for different values of  $D1$

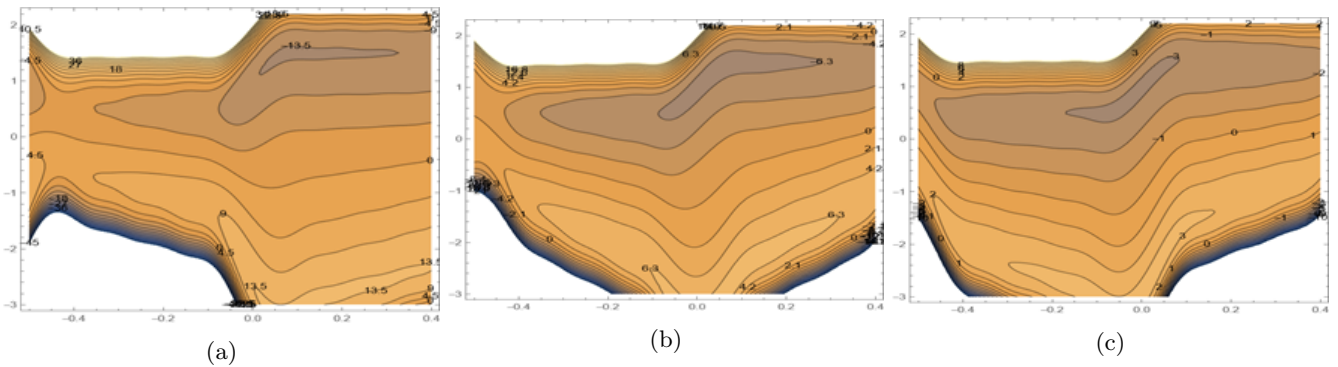


Figure 9: stream lines for different values of  $\phi$  (a)  $\phi = \text{Pi}/6$  (b)  $\phi = \text{Pi}/2$  (c)  $\phi = 3\text{Pi}/4$

$\phi$  because the difference between initial and final concentration is few, it increases the concentration of molecules and thus increases the pressure. Prandtl number  $Pr$  has little effect on the pressure gradient due to their appearance within limits. The pressure gradient decreases with increasing value of the amplitude of the wave number  $a$ . In the Brownian motion parameter  $Nb$  The pressure gradient increases with the increasing value of the  $Nb$  because of the few kinematic viscosity. The pressure gradient decreases with the increasing value of thermophoresis parameters  $Nt$  this means that the concentration decreases due to the velocity increase which results in a little pressure. The



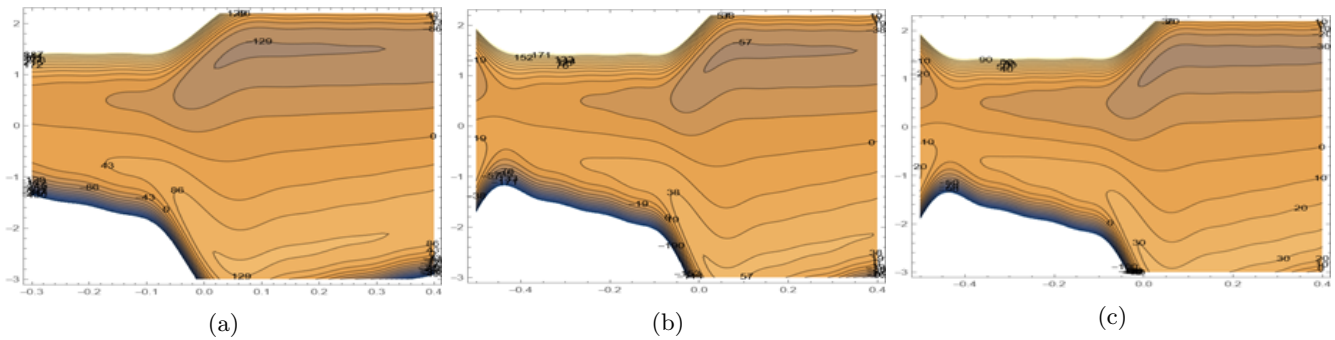


Figure 10: stream lines for different values of  $d(a)$   $d = 1.4$  (b)  $d = 1.6$  (c)  $d = 1.8$

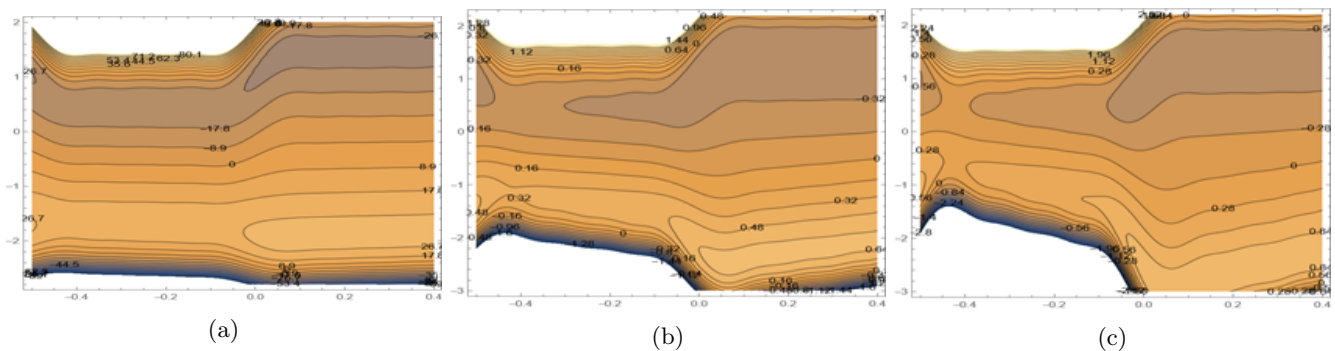


Figure 11: stream lines for different values of  $b(a)$   $b = 0.1$  (b)  $b = 0.5$  (c)  $b = 0.9$

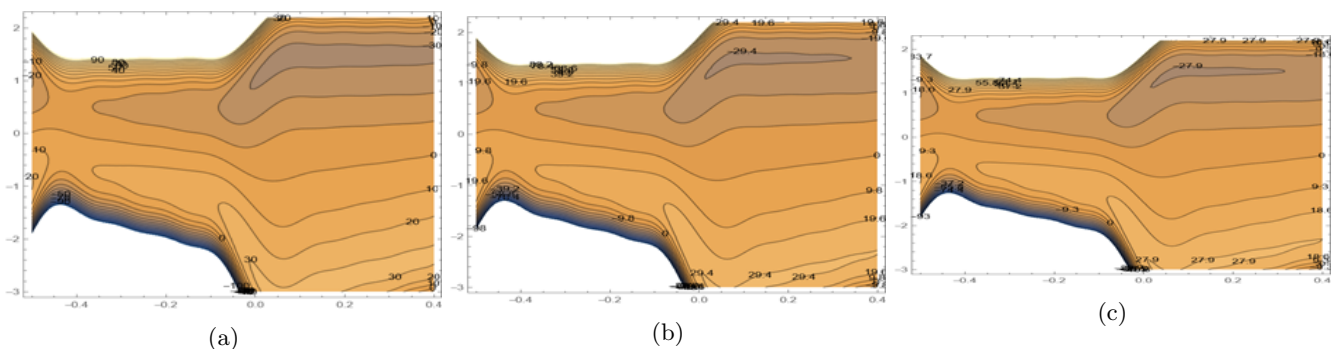


Figure 12: stream lines for different values of  $\gamma(a)$   $\gamma = 2.5$  (b)  $\gamma = 2.7$  (c)  $\gamma = 2.9$

pressure gradient is increasing with the increasing value of the nanoparticle Grashof number  $Br$ , the width number  $d$ , discharge  $Q$ , and the couple stress parameter  $\gamma$ . The pressure gradient is increasing with the increasing value of the local temperature Grashof number  $Gr$ . This occurs as a result of the effect of the quotient multiplying the length wave in the viscosity. The pressure gradient is increasing with the increasing value of the porosity parameter  $D_1$ . Due to increased permeability of molecules. The pressure gradient decreases with the increasing value of the amplitude of the wave number  $b$ . In the magnetic parameter  $M$  the pressure gradient decreases with the increasing value  $M$  because of low viscosity.

### 5.4 Stream line

Trapping for various values of  $\phi, Pr, a, Nb, Nt, d, b, Gr, Br, Q, M, \gamma$  and  $D_1$  can be seen through figure (3.36) (3.25). The effect of the concentration  $\phi$  it has been noticed that the bolus increases in size in the upper wall with increasing  $\phi$  but in the lower wall the bolus decreases in size with increasing  $\phi$ . The Prandtl number  $Pr$ , Brownian motion parameter  $Nb$ , thermophoresis parameters  $Nt$ , local temperature Grashof number  $Gr$ , width number  $d$ , and nanoparticle Grashof number  $Br$  have little effect on the stream line. With an increase in the amplitude of the wave number  $a$ , it was seen that the size of the bolus decreased in the upper walls, and in the lower walls the bolus increases in size with

increasing  $a$ . In the amplitude of the wave number  $b$ , the size of boulders is increasing with increasing value of  $b$ , in upper walls and in the lower walls the size of boulders decreases with increased values of  $b$ . The effect of the magnetic parameter  $M$  it has been the size of boulders is increasing with increasing value of  $M$  in upper walls, and in the lower walls, the size of boulders decreases with increased value of  $M$ . The effect of the couple stress  $\gamma$  it is found that the boulders increase in size with increased value of  $\gamma$  in upper walls but in the lower walls, the size of boulders decreases with increased value of  $\gamma$ . The effect of porosity parameter  $D1$  it has been the size of boulders is decreases with increasing value of  $D1$  in the upper walls but in the lower walls the size of boulders is increases with increasing value of  $D1$ .

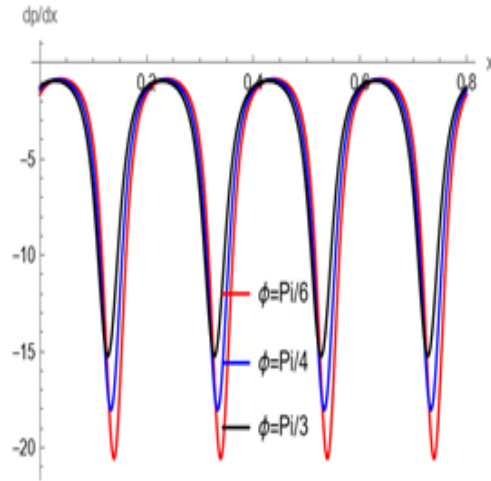


Figure 13: variation of pressure gradient  $dp/dx$  with  $x$  for different values of  $\phi$

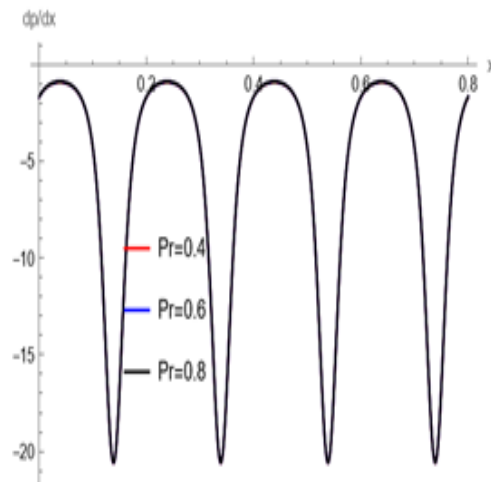


Figure 14: variation of pressure gradient  $dp/dx$  with  $x$  for different values of  $Pr$

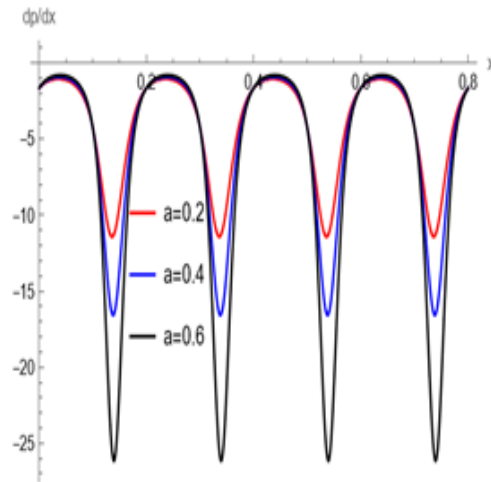


Figure 15: variation of pressure gradient  $dp/dx$  with  $x$  for different values of  $a$

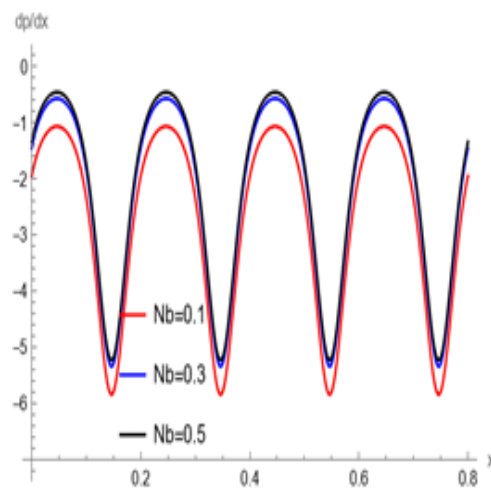


Figure 16: variation of pressure gradient  $dp/dx$  with  $x$  for different values of  $Nb$

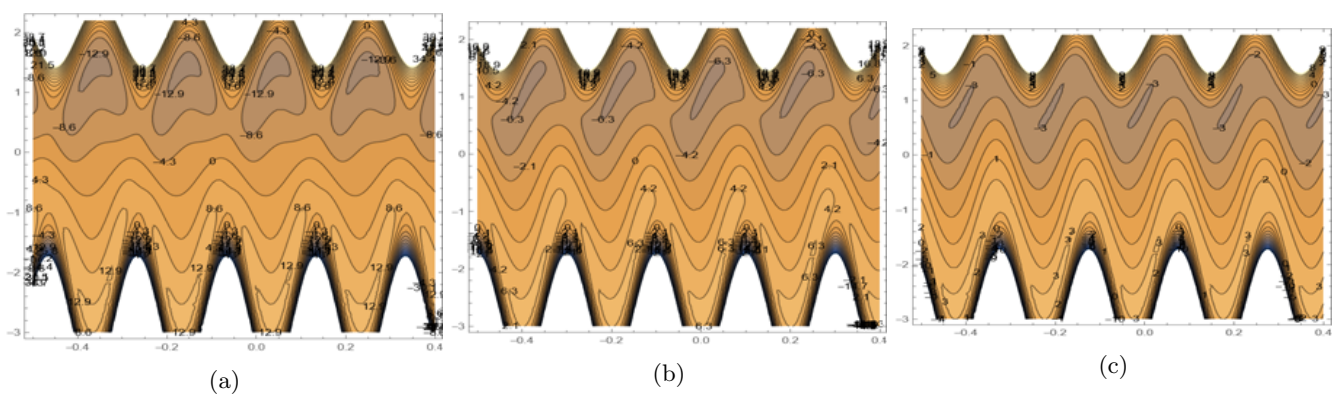


Figure 17: stream lines for different values of  $\phi$  (a)  $\phi = \pi/6$  (b)  $\phi = \pi/2$  (c)  $\phi = 3\pi/4$

## 6 Conclusions

In this section, we investigated the effect of MHD and porous media on the peristaltic flow of a couple of stress fluids in an asymmetric channel for different types of walls, Then the exact solutions of the pressure equation and

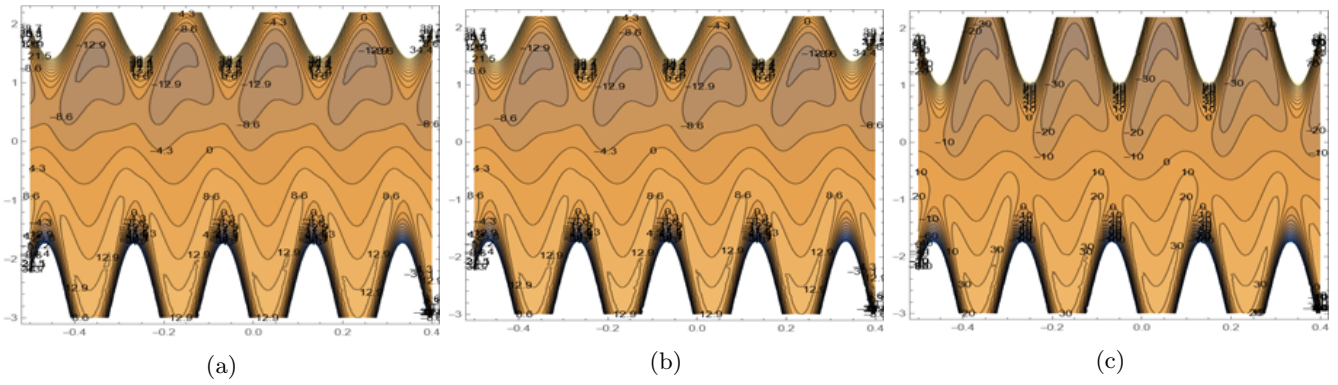


Figure 18: stream lines for different values of  $a(a) a = 0.5$  (b)  $a = 0.7$  (c)  $a = 0.9$

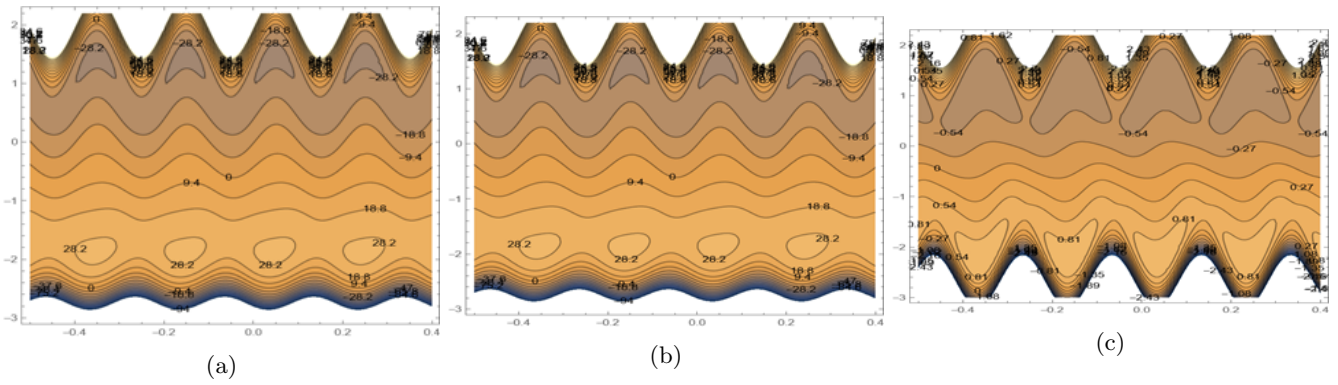


Figure 19: stream lines for different values of  $b(b) b = 0.1$  (b)  $b = 0.3$  (c)  $b = 0.5$

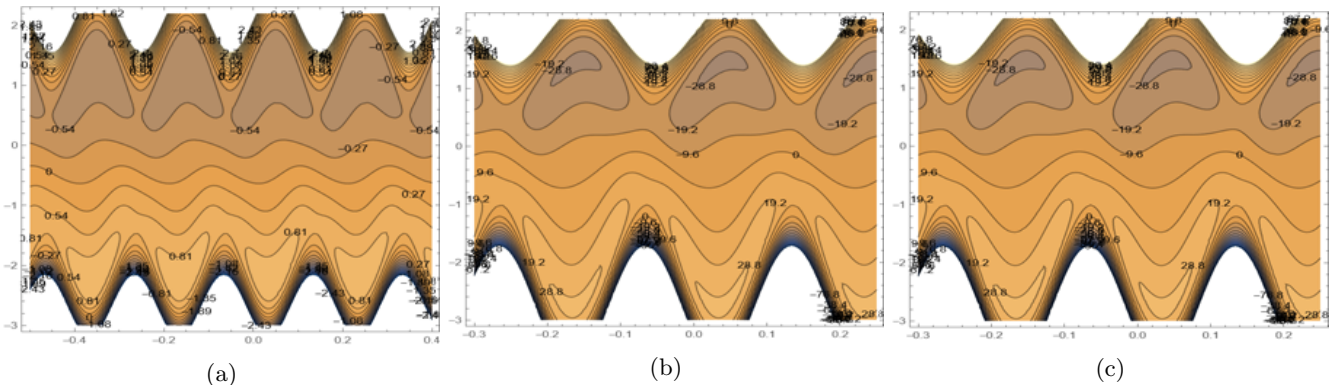


Figure 20: stream lines for different values of  $M(a) M = 0.2$  (b)  $M = 0.4$  (c)  $M = 0.6$

stream function will be taken. the effects of the concentration  $\phi$ , Prandtl number  $Pr$ , amplitude of the wave number  $a$  &  $b$ , Brownian option parameter  $Nb$ , thermophoresis parameters  $Nt$ , width number  $d$ , couple stress  $\gamma$ , discharge  $Q$ , nanoparticle Grashof number  $Br$ , magnetic parameter  $M$ , and porosity parameter  $D1$  are also investigated in details, it found that:

- 1-  $Pr$  has little effect on the pressure gradient trapezoidal wave, and multisinusoidal wave . In trapezoidal wave
- 2- The pressure gradient is increasing with the increasing value of  $\phi, d, Q, \gamma, Gr, D1$ .
- 3- The pressure gradient increases with increasing  $a$ , after the point  $x = [0.5]$  the pressure gradient decreases with increasing amplitude of the wave number  $a$ . The pressure gradient decreases with the increasing values  $Nt, M, b$ .
- 4- The size of boulds is increasing with increasing values of  $\phi, b, d, \gamma$  in upper walls and in the lower walls the size of boulds decreases with increased values of  $\phi, b, d, M, \gamma$ .

- 5- The size of boulds decreases with increasing of value  $D1$  in the upper walls but in the lower walls, the size of boulds increases with increasing value  $D1$
- 6-  $Pr, Nb, Nt, Gr, Br$  have little effect on the stream line. In multisinusoidal wave
- 7- The pressure gradient is increasing with the increasing value of  $\phi, Nb$ .
- 8- The pressure gradient is decreasing with the increasing value of  $a$ .
- 9- The size of boulds is increasing with increasing values of  $\phi, b, M$  in upper walls and in the lower walls the size of boulds decreases with increased values of  $\phi, b, M$ .
- 10- The size of boulds decreases with increasing of value  $a$  in the upper walls but in the lower walls the size of boulds increases with increasing value  $a$
- 11-  $Pr, Nb, Nt, Gr, d, Br$  have little effect on the stream line.

## References

- [1] F.M. Abbasi, A. Alsaedi and T. Hayat, *Mixed convective heat and mass transfer analysis for peristaltic transport in an asymmetric channel with Soret and Dufour effects*, J.Cent. South Univ. **12** (2014), 4585–4591.
- [2] F.M. Abbasi, M. Gul and S.A. Shehzad, *Effectiveness of temperature-dependent properties of Au, Ag, Fe<sub>3</sub>O<sub>4</sub>, Cu nanoparticles in peristalsis of nanofluids*, Int. Commun. Heat Mass Transf. **116** (2020), 104651.
- [3] F.M. Abbasi and S.A. Shehzad, *Convective thermal and concentration transfer effects in hyhydromagnetic peristaltic transport with Ohmic heating*, J. Adv. Res. **8** (2017)655-661.
- [4] Akram, Safia, F. Afzal and Q. Afzal. *Impact of nanofluids and magnetic field on the peristaltic transport of a couple stress fluid in an asymmetric channel with different wave forms*, Thermal Sci. **24** (2020), no. 2, 1407–1414.
- [5] N. Ali, M. Sajid, T. Javed and Z. Abbas, *Heat transfer analysis of peristaltic flow in a curved channel*, Int. J. Heat Mass Transf. **53** (2010), 3319–3325.
- [6] A. Bhattacharyya, R. Kumar and G.S. Seth, *Capturing the features of peristaltic transport of a chemically reacting couple stress fluid through an inclined asymmetric channel with Dufour and Soret effects in presence of inclined magnetic field*, Indian J. Phys. **95** (2021), no. 12, 2741–2758.
- [7] M.M. Bhatti, R. Ellahi and A. Zeeshan, *Study of variable magnetic field on the peristaltic flow of Jeffrey fluid in a non-uniform rectangular duct having compliant walls*, J. Mol. Liq. **222** (2016), 101–108.
- [8] S.U.S. Choi, *Enhancing thermal conductivity of fluid with nanofluids*, D.a. Siginer, H. P. Wang (Eds.), *developments and applications of non Newtonian flows*, ASME J. Heat Transfer **66** (1995), 99–105
- [9] S.U.S. Choi and J.A. Eastman, *Enhancing thermal conductivity of fluids with nanoparticles ASME*, Int. Mech. Engin. Cong. Expos., 1995, pp. 12–17.
- [10] E.F. Elshehawey , N.T. Eldabe , E.M. Elghazy and A. Ebaid, *Peristaltic transport in an asymmetric channel through a porous medium*, Appl. Math. Comput. **182** (2006), no. 1, 140–150.
- [11] T. Hayat, N. Aslam, M.I. Khan and A. Alsaedi, *Mixed convective peristaltic flow of Carreau–Yasuda fluid in an inclined symmetric channel*, Microsyst. Technol. **25** (2019), 609–620
- [12] T. Hayat, N. Ali and S. Asghar, *Hall effects on peristaltic flow of a Maxwell fluid in a porous medium*, Phys. Lett. A **363** (2007), 397–403.
- [13] S.U. Khan and S.A. Shehzad, *Electrical MHD Carreau nanofluid over a porous oscillatory stretching surface with variable thermal conductivity: applications of thermal extrusion system*, Phys. A. Stat. Mech. Appl. **550** (2020), 124132.
- [14] T.W. Latham, *Fluid Motion in a Peristaltic Pump*, Master's Thesis Massachusetts Institute of Technology, Cambridge, 1966.
- [15] M.J. Martinez and D.F. McTigue, *Modeling in Nuclear Waste Isolation: Approximate Solutions for Flow in Unsaturated Porous Media*, Wheeler M.F. (eds) Environmental Studies. The IMA Volumes in Mathematics and its Applications, vol 79. Springer, New York, NY, 1996.

- 
- [16] K.J. Qabas and M.A. Ahmed, *Influence of MHD and porous media on peristaltic transport for nanofluids in an asymmetric channel*, Iraqi J. Sci. **64** (2022), no. 3, 2312–1637
- [17] A.H. Shapiro, M.Y. Jaffrin and S.L. Weinberg, *Peristaltic pumping with long wavelengths at low Reynolds number*, J. Fluid Mech. **37** (1969), 799–825.
- [18] D. Tripathi, *Study of transient peristaltic heat flow through a finite porous channel*, Math. Comput. Model. **57** (2013), 1270–1283.